Vibrational Spectroscopy of Protonated Imidazole and its Complexes with Water Molecules: Ab Initio Anharmonic Calculations and Experiments†

Adeyemi A. Adesokan,‡ Galina M. Chaban,§ Otto Dopfer,|| and R. Benny Gerber§,*,†,‡,+

Department of Chemistry, University of California at Irvine, Irvine, California 92697, NASA Ames Research Center, Mail Stop T27B-1, Moffet Field, California 94035, Institut für Optik und Atomare Physik, Technische Universität Berlin, Hardenbergstrasse 36, 10623 Berlin, Germany, Department of Physical Chemistry and The Fritz Haber Research Center, The Hebrew University of Jerusalem, Jerusalem 91904, Israel

Received: January 30, 2007; In Final Form: April 4, 2007

The results of anharmonic frequency calculations on neutral imidazole ($C_3N_2H_4$, Im), protonated imidazole (ImH^+), and its complexes with water $(ImH^+)(H_2O)_n$, are presented and compared to gas phase infrared photodissociation spectroscopy (IRPD) data. Anharmonic frequencies are obtained via ab initio vibrational self-consistent field (VSCF) calculations taking into account pairwise interactions between the normal modes. The key results are: (1) Prediction of anharmonic vibrational frequencies on an MP2 ab initio potential energy surface show excellent agreement with experiment and outstanding improvement over the harmonic frequencies. For example, the ab initio calculated anharmonic frequency for $(ImH^+)(H_2O)N_2$ exhibits an overall average percentage error of 0.6% from experiment. (2) Anharmonic vibrational frequencies calculated on a semiempirical potential energy surface fitted to ab initio harmonic data represents spectroscopy well, particularly for water complexes. As an example, anharmonic frequencies for $(ImH^+)H_2O$ and $(ImH^+)(H_2O)_2$ show an overall average deviation of 1.02% and 1.05% from experiment, respectively. This agreement between theory and experiment also supports the validity and use of the pairwise approximation used in the calculations. (3) Anharmonic coupling due to hydration effects is found to significantly reduce the vibrational frequencies for the NH stretch modes. The frequency of the NH stretch is observed to increase with the removal of a water molecule or replacement of water with N_2. This result also indicates the ability of the VSCF method to predict accurate frequencies in a matrix environment. The calculation provides insights into the nature of anharmonic effects in the potential surface. Analysis of percentage anharmoncity in neutral Im and ImH^+ shows a higher percentage anharmonicity in the NH and CH stretch modes of neutral Im. Also, we observe that anharmonicity in the NH stretch modes of ImH^+ have some contribution from coupling effects, while that of neutral Im has no contribution whatsoever from mode−mode coupling. It is concluded that the incorporation of anharmonic effects in the calculation brings theory and experiment into much closer agreement for these systems.

I. Introduction

Imidazole ($C_3N_2H_4$, henceforth denoted Im) is an essential component of nucleic acid bases such as adenine and guanine and occurs as a functional group in the amino acid residue histidine (His). By virtue of its unique ring structure which allows it to act as both a proton donor and acceptor, Im and its protonated and hydrogen-bonded derivatives play an important role in enzymatic reaction mechanisms, proton transport pathways, and electron transfer in photosynthesis.[1−4] To acquire a detailed understanding of principles that underlie the action of Im in these processes, thorough knowledge of its intermolecular potential energy surface (PES) and surrounding aqueous environment is essential. For microhydrated imidazole complexes in particular, a rather small range of experimental and theoretical studies has been able to contribute immensely to the general elucidation of the mechanistic details of solvent and charge assisted proton shuttle properties of histidine residues in protein active sites.[5−9] These studies have also been able to provide direct information on the acidity of the Im NH and OH bonds and also on the structure and energy of the preferred microhydration motif.[6]

Vibrational spectroscopy is a sensitive probe of molecular properties. It is in particular sensitive to the PES, and contains information on the interactions between different vibrational modes. Recent progress in the field of experimental vibrational spectroscopy which has allowed for the study of biological molecules complexed with helium nanodroplets and also in the gas phase, has made available high-resolution spectroscopic data.[10−32] This in turn has led to a deeper and more accurate view of the role of forces and dynamics in fundamental biological processes.[33] For example, the application of techniques such as sensitive infrared photodissociation spectroscopy (IRPD) to isolated and microsolvated protonated aromatic molecules, protonated peptides, and proton bound dimers of amino acids have provided invaluable insight into the dissociation behavior, preferred protonation sites and the influence of microsolvation on nonpolar environments.[6,14−18] Furthermore, infrared experiments have made possible the determination of amino acid and peptide conformations and also the exploration

† Part of the "Roger E. Miller Memorial Issue".
* Corresponding author. E-mail: benny@fh.huji.ac.il.
‡ University of California, Irvine.
§ NASA Ames Research Center.
|| Technische Universität Berlin.
+ The Hebrew University of Jerusalem.

10.1021/jp070785w CCC: $37.00
Published on Web 05/15/2007

of nucleic acid base tautomerization and pairing.[19−25] These experimental advances have coincided with an increased availability of powerful theoretical approaches and algorithms and has thus lead to a rich synergy between experimental measurement and ab initio calculation which has resulted in the mining of previously underutilized spectroscopic information.

Although theoretical spectroscopic calculations aiming at interpreting experimental data have been carried out for neutral Im,[5,34] so far only a few theoretical studies on $(ImH^+)(H_2O)_n$ clusters have been reported and none have included an explicit anharmonic description of the vibrational PES.[6−9] Frequency scaling has been used in most cases, but since strong anharmonic effects can be expected for at least the hydrogen bonded interactions, the need for an explicit description of anharmonicity in these calculations is essential. In this work we present the first computational study of the anharmonic vibrational spectroscopy of neutral Im and $ImH^+(H_2O)_n$ by means of the vibrational self-consistent field method (VSCF) and its variants.[35−42] The calculations are for a multidimensional PES of a semiempirical electronic structure theory, improved by input from high level ab initio calculations. The advantages of the VSCF method for the purpose of this study are as follows: (a) The method has proven to be of good accuracy in a range of applications to realistic systems. For the systems featured in this study, an average overall percentage error of less than 1% was observed for all modes calculated. (b) VSCF directly employs potentials obtained from electronic structure theory. (c) Computationally, the method can be directly applied with ab initio potentials for large systems.[38] The importance of direct ab initio vibrational calculations is great in this case, since fitting of ab initio potentials for large systems is very complicated.

Finally, anharmonic interactions are not only critical to obtaining a high degree of agreement between theory and experiment but also bear relevance to the characteristics of vibrational energy flow within the system. Thus, the anharmonic calculations not only validate the PES but also provide information on the coupling characteristics especially in the hydration stages. With this in view, we examine the coupling character between important vibrational modes in the systems studied.

The outline of this paper is as follows: In the methods section, we present the experimental methodology and an overview of the VSCF method. In the results and discussion section, we consider the molecular geometries of the systems studied and also present a comparison of theory with experiment, with particular focus on the importance of the semiempirical and higher level surfaces used. This is followed by comments on the difference between the PES of hydrogen bonded and non hydrogen-bonded imidazole and the role of single mode and coupled anharmonic effects in the systems studied. Finally, we close with concluding remarks on the need for accurate anharmonic calculations in step with advanced experimental spectroscopic techniques as a means of further understanding spectra and biochemical reactions.

II. Methodology

A. The Vibrational Self-Consistent Field Method (VSCF). In this study anharmonic interactions, including coupling between different modes, are obtained using the VSCF approach and its variants.[35,39] These methods are implemented in the GAMESS suite of codes, and the calculations here used this package.[43] This technique can be applied to potential surfaces from electronic structure methods and is reasonably accurate for a variety of systems.[36−42] Unlike analytic force fields, the potential surface is generated on grid points and is not available as an analytic function. Since VSCF has been discussed extensively in the literature, here we give only a brief overview of the method.[36−42,44]

The VSCF method is used to solve the vibrational Schroedinger equation to obtain vibrational wavefunctions in mass weighed normal coordinates. At the lowest level, VSCF is a separable but anharmonic approximation. The vibrational wavefunctions are computed from mean-field potentials, that represent the effects of the other vibrations in a given mode.

In practicality, the main computational difficulty in VSCF involves the numerical solution of rather costly multidimensional integrals. We have found it advantageous to represent the potential as a sum of terms that include single-mode potentials $V_j^{\mathrm{diag}}(Q_j)$, and interactions between pairs of normal modes $W_{ij}^{\mathrm{coup}}(Q_i,Q_j)$. Two types of anharmonic interactions are thus taken into account in the VSCF framework: (1) the intrinsic anharmonicity which is given by the single mode or diagonal potentials and does not involve coupling with other modes and (2) anharmonicity due to mode−mode coupling. Contributions to the potential from interactions of triplets and quartets (or higher order interactions) of normal modes are neglected, and the potential is thus written as

$$V(Q_1,...,Q_N) = \sum_{j=1}^{N} V_j^{\mathrm{diag}}(Q_j) + \sum_i \sum_{j>i} W_{ij}^{\mathrm{coup}}(Q_i,Q_j) \quad (1)$$

Although this approximation has proven to be successful in many cases, it cannot be taken for granted and must be tested for each application.[36−37,40,44]

The simplest separable VSCF approximation may not be of sufficient accuracy for comparison with experiments, and corrections for correlations between different vibrational modes are required. An extension of VSCF using this approach is the correlation corrected VSCF (CC-VSCF) method,[35] which includes the non-separability of the vibrational wavefunction by perturbation theoretical corrections. Another variant of VSCF is the vibrational configuration interaction VSCF (VCI-VSCF) method, which includes corrections for certain degeneracies between different vibrational modes.[39]

B. Potential Functions. Anharmonic vibrational spectroscopy calculations were carried out on an improved semiempirical (PM3) potential energy surface (PES). PM3 is one of several modified NDDO approximation methods (neglect of diatomic differential overlaps methods).[45] Unfortunately, however, while computationally efficient, standard PM3 is not sufficiently accurate. Our approach in improving PM3 in this context was originally proposed and implemented for a large range of biomolecules by Brauer et al. and has been validated by subsequent studies.[37,40,44] The method involved changing the harmonic force constants so as to agree with harmonic force constants obtained using the MP2 electronic structure method and the Dunning-Hay double-ζ polarized (DZP) basis[46−48] as implemented in the GAMESS electronic structure package. That is the (improved) PM3 level is designed to agree with MP2 level at the harmonic approximation. This is accomplished by introducing a scaling of PM3, such that

$$V_{\mathrm{scaled}}(Q_1,...,Q_n) = V_{\mathrm{PM3}}(\lambda_1 Q_1,.....\lambda_n Q_n) \quad (2)$$

where V_{scaled} is a scaled potential, V_{PM3} is the PM3 potential surface, and Q_j is the jth normal mode coordinate. The scale factor λ_i is determined by the ratio

$$\lambda_i = \omega_{\mathrm{MP2},i}/\omega_{\mathrm{PM3},i} \quad (3)$$

where $\omega_{MP2,i}$ is the *i*th harmonic frequency obtained by the MP2 method, while $\omega_{PM3,i}$ represents the corresponding harmonic frequency obtained by PM3. The λ_j factors were then entered into the potential surface calculation in the VSCF portion of the GAMESS program. Thus, the standard PM3 potential surface in normal coordinates is modified by scaling of each normal-mode coordinate Q_j with the scale factor λ_j. While the scaling is expected to improve the potential at the harmonic level, since MP2 is superior to standard PM3, the effect of the scaling beyond this approximation can only be tested by the predictions obtained with the scaled potential.

The preconditions for carrying out this scaling procedure include similarities in the MP2 and PM3 structures, and a close correspondence in the nature of the vibrational modes that are being scaled. The proposed scaling makes intuitive sense only if the PM3 normal mode being scaled is similar to the MP2 mode used in scaling. Thus as a test of similarity, a one-to-one correspondence between the normal modes from the two methods (MP2 and PM3) is obtained as follows: Initially, the dot products of the normal mode vectors from PM3 and those from MP2/DZP are compared in order to find the most similar modes. Typically an overlap whose absolute value is between 0.6 and 1.0 indicates a likely similarity between normal modes. Next the motions are visually compared using the MacMolPlt program.[49] A visual comparison was required since the direction of the normal mode vectors is not unique and occasionally, modes involving motions of several types can be similar, yet have partial cancellation.

C. Experimental Methodology. IRPD spectra of weakly bound $(ImH^+)(H_2O)_n$ clusters were recorded in a tandem quadrupole mass spectrometer (QMS1/2) coupled to an ion source and an octopole ion trap.[7,50] The ion source combines a pulsed supersonic molecular beam expansion with electron ionization. The $(ImH^+)(H_2O)_n$ cluster ions produced were mass selected by QMS1 and irradiated in the adjacent octopole ion guide with a tunable IR laser pulse generated by an optical parametric oscillator laser system. Resonant vibrational excitation of $(ImH^+)(H_2O)_n$ induced the evaporation of a single water ligand. The produced $(ImH^+)(H_2O)_{n-1}$ fragment ions were selected by QMS2 and monitored as a function of the IR laser pulse to obtain the IRPD spectrum of $(ImH^+)(H_2O)_n$. Experimental frequencies for bare ImH^+ were obtained by extrapolation from $(ImH^+)L_n$ data (L = Ar, N_2) to zero solvation (n = 0).[7] For further details about the experimental procedure, the reader is referred to ref 7.

III. Results and Discussion

A. Molecular Geometry. The optimized geometries of the Im complexes resulting from the ab initio optimizations had bond lengths consistent with those obtained from experiments and previous calculations.[6,7,34] Figures 1 and 2 show the equilibrium geometry and atom numbering scheme of ImH^+ and $(ImH^+)(H_2O)N_2$. Comparison of the computed geometrical parameters with those from experiments is presented in the Supporting Information. The bond lengths and the angles obtained theoretically via MP2 methods are seen to be in agreement with earlier experimental work. For example, the neutral Im bond lengths show a mean percentage deviation of about 0.002% from experiment. The mean percentage deviation from experiments for the bond angles in neutral Im is about 0.0002%.

Difficulties with the use of PM3 for describing hydrogen-bonded complexes have been discussed by several authors and have been attributed to the inadequate description of the rotational barrier of the amide bond by PM3.[51,52] The impact of errors due to PM3 can be reduced through the application of ab initio scaling methods to PM3.[51] For all systems studied, we observe good agreement between ab initio and PM3 calculated bond distances. In most cases PM3 is within 0.04 Å of ab initio distances. An exception to this rule are the CN bond distances, which is primarily associated with hydrogen-bonding portions of the guanine ring. The PM3 bond angles are also in general agreement with the ab initio data, with the largest deviations observed around the CN bonds. This observation concerning PM3 is consistent with that of earlier studies on base pairs by Brauer et al.[44]

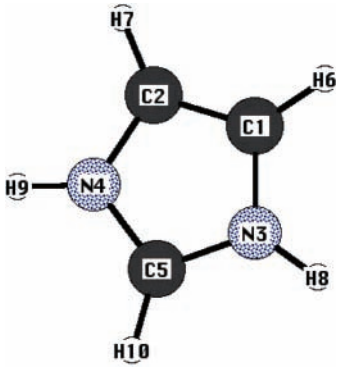

Figure 1. Equilibrium structure and atom numbering scheme of ImH^+.

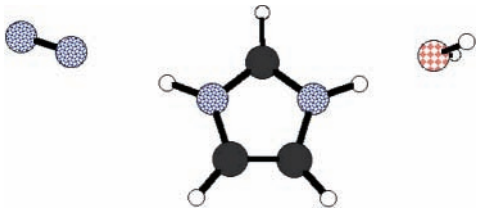

Figure 2. Equilibrium structure of $(ImH^+)(H_2O)N_2$.

B. Vibrational Frequencies—Comparison of Theory to Experiment. The anharmonic vibrational frequencies of the normal modes of vibration of neutral Im, ImH^+, $(ImH^+)H_2O$, $(ImH^+)(H_2O)_2$, and $(ImH^+)(H_2O)N_2$ were calculated by means of VSCF and compared to experimental frequencies. Tables 1−5 show comparisons of VSCF anharmonic frequencies, harmonic frequencies and IRPD experiments. For all systems calculated VSCF anharmonic frequencies compare better to experiments than harmonic frequencies.

1. Pure ab Initio versus Experiment. I. $(ImH^+)(H_2O)N_2$. Generally, the ab initio VSCF calculations carried out for $(ImH^+)(H_2O)N_2$ give the best overall agreement with experiment, with an average overall deviation of 0.6% from experiment and a major portion of the VSCF frequencies for the $(ImH^+)(H_2O)N_2$ species having a deviation of 0.2% or less from the IRPD experimental frequencies. We see here the power of VSCF and the usefulness of the pairwise approximation especially when the calculations are based on a pure ab initio surface. (See Table 1). Ab initio VSCF anharmonic frequencies shows particularly good agreement with IRPD experiments for the water bound NH stretch. For this mode an ab initio VSCF frequency of 2890 cm^{-1} is computed compared to experiment at 2897 cm^{-1}. The accurate result from the ab initio VSCF shows that VSCF is able to estimate to a very high degree of accuracy the frequencies of hydrogen-bonded systems. In Table 1 we also observe very good agreement for the ab initio VSCF anharmonic frequency of the N_2 bound NH stretch, where a value of 3388 cm^{-1} is calculated in comparison to a value of 3404 cm^{-1} from IRPD experiments (corresponding to an error

TABLE 1: $(ImH^+)(H_2O)N_2$ Assignment and Comparison of Theoretical Harmonic and Anharmonic Frequencies in Wave Numbers to Those Obtained from Experiments

PM3 mode	harmonic (MP2/DZP)	CC-VSCF (MP2/DZP)	IRPD	mode description
1	3884	3648	3639	water sym stretch
2	4011	3696	3723	water assym stretch
3	3217	2890	2897	NH stretch (toward water)
4	3587	3388	3404	NH stretch (toward N_2)
5	3380	3205	app 3172	C1H stretch, C2H stretch
6	3372	3165	app 3172	CH stretch
7	3392	3221	app 3172	C5H stretch

TABLE 2: $(ImH^+)(H_2O)N_2$ Assignment and Comparison of Theoretical Harmonic and Anharmonic Frequencies in Wave Numbers to those Obtained from Experiments

PM3 mode	harmonic (MP2/DZP)	CC-VSCF (Imp. PM3)	IRPD	mode description
1	3884	3684	3639	water sym stretch
2	4011	3747	3723	water assym stretch
3	3217	2986[a]	2897	NH stretch (toward water)
4	3587	3317	3404	NH stretch (toward N_2)
5	3380	3186	app 3172	C1H stretch, C2H stretch
6	3372	3175[a]	app 3172	CH stretch
7	3392	3199[a]	app 3172	C5H stretch

[a] VCI−VSCF.

of 0.44% for this mode). This high degree of accuracy is maintained by ab initio VSCF for this NH stretch mode in the presence or absence of a hydrogen bonded interaction with this NH bond.

2. Ab Initio Improved PM3 VSCF versus Experiment (Complex Systems). I. $(ImH^+)(H_2O)N_2$. An overall average percentage deviation from experiment of 0.9% was observed for $(ImH^+)(H_2O)N_2$ when anharmonic frequencies were calculated on an ab initio improved PM3 surface. Compared to ab initio VSCF, scaled VSCF anharmonic frequencies does not perform as well for the N_2-bound NH stretch mode, as an anharmonic frequency of 3317 cm^{-1} is calculated compared to experiment at 3404 cm^{-1}. Thus, an average error of 0.44% for ab initio VSCF compared to an error of 2.5% for scaled VSCF is observed for this mode. It is evident from these results that ab initio VSCF performs better especially for this NH stretch mode. On the other hand, the accuracy of the scaled VSCF frequencies is found to significantly increase for this NH stretch mode as we move from hydrogen bonded to non hydrogen-bonded systems. Excellent agreement is seen also for the CH stretch modes in the VSCF calculations carried out on the improved PM3 surface. The deviation from the experiment for these modes in scaled VSCF is 0.4% compared to 0.9% in ab intio VSCF. (See Table 2)

II. $(ImH^+)(H_2O)_2$. As nucleotides function in aqueous environments, water molecules were added to ImH^+ to simulate a microhydrated environment. With the replacement of N_2 by H_2O, we see the overall deviation of scaled VSCF from experimental frequencies to be about 0.95%. Particularly good agreement between scaled VSCF results and IRPD experiments is observed for the water symmetric stretch mode. (See Table 3) VSCF predicted a frequency of 3642 cm^{-1} compared to 3635 cm^{-1} by IRPD, resulting in a deviation of 0.2% for this mode. Excellent agreement is also seen for the CH stretch (mode 8), where a VSCF value of 3177 cm^{-1} was predicted in comparison to 3170 cm^{-1} from IRPD. The VSCF accuracy for the water-bound NH stretch changed from 3% in $ImH^+(H_2O)N_2$ to 2.3% in $(ImH^+)(H_2O)_2$. This slight improvement may point to the fact the PM3 may not be well suited for the characterization of systems in a matrix environment.

TABLE 3: $(ImH^+)(H_2O)_2$ Assignment and Comparison of Theoretical Harmonic and Anharmonic Frequencies in Wave Numbers to those Obtained from Experiments

PM3 mode	harmonic (MP2/DZP)	VCI-VSCF	IRPD[a]	mode description
1	4022	3779		water assym stretch
2	4012	3776	3718	water assym stretch
3	3890	3642	3635	water sym stretch
4	3881	3624		water sym stretch
5	3297	3094[b]		N3H stretch (water bound)
6	3240	2967	2900	N4 H stretch (water bound)
7	3402	3202[b]	app 3170	C1H stretch and C2H stretch
8	3379	3177	app 3170	C1H stretch and C2H stretch
9	3361	3186	app 3170	CH stretch and NH stretch

[a] Reference 7. [b] CC-VSCF.

TABLE 4: $(ImH^+)H_2O$ Assignment and Comparison of Theoretical Harmonic and Anharmonic Frequencies in Wave Numbers to those Obtained from Experiments

PM3 mode	harmonic (MP2/DZP)	CC-VSCF (Imp. PM3)	IRPD[a]	mode description
1	3877	3722	3710	water assym stretch
2	4005	3657	3630	water sym stretch
3	3701	3490[b]	3468	N3H stretch
4	3162	2956[b]	2895	N4H stretch (water bound)
5	3408	3242[b]	app 3170	CH sym stretch
6	3388	3175	app 3170	CH assym stretch
7	3363	3207[b]	app 3170	C5H10 stretch

[a] Reference 7. [b] VCI-VSCF.

TABLE 5: ImH^+ Assignment and Comparison of Theoretical Harmonic and Anharmonic Frequencies in Wave Numbers to those Obtained from Experiments

PM3 mode	harmonic (MP2/DZP)	CC-VSCF (Imp. PM3)	IRPD[a]	mode description
1	3705	3431	app 3470	NH stretch
2	3660	3424	app 3470	NH stretch
3	3401	3225	app 3170	CH sym stretch
4	3379	3174	app 3170	CH assym stretch
5	3357	3136[b]	app 3170	C5H10 stretch

[a] Reference 7. [b] VCI-VSCF.

III. $(ImH^+)H_2O$. With the removal of one of the water molecules hydrogen bonded to NH, the overall average error of scaled VSCF increased from 0.95% for $(ImH^+)(H_2O)_2$ to 1.02% for $(ImH^+)H_2O$. Particularly good agreement is observed for the water asymmetric stretch where a VSCF anharmonic frequency of 3722 cm^{-1} is predicted compared to an experimental frequency at 3710 cm^{-1} (representing a deviation of 0.3% from experiment). (See Table 4). Similar to the case of $(ImH^+)(H_2O)N_2$, scaled VSCF predicts the symmetric water stretch well. Excellent agreement is also seen for the N3H stretch where a deviation of 0.6% is observed from IRPD experiment. This is not the case, however, for the water bound N4H stretch where VSCF predicts a frequency of 2956 cm^{-1} compared to a value of 2895 cm^{-1} from IRPD, resulting in an overall percentage deviation of 2.1% from experiment.

3. Ab intio Improved PM3 versus Experiment (Noncomplex Systems). I. ImH^+. The overall deviation of scaled VSCF anharmonic frequencies from experiment for ImH^+ was about 1.05%, with the best agreement between theory and experiment observed for the asymmetric CH stretch mode 4. VSCF predicts a value of 3174 cm^{-1} compared to 3170 cm^{-1} from experiments.(Table 5.) With a loss of hydrogen-bonded water, the frequencies of the NH stretch modes are observed to increase. VSCF predicts this increase accurately with an average deviation of 1.3% for the NH stretches.

TABLE 6: Im. Assignment and Comparison of Theoretical Harmonic and Anharmonic Frequencies in Wave Numbers to those Obtained from Experiments

PM3 mode	harmonic (MP2/DZP)	CC-VSC F	FTIR expt[34]	FTIR vapor[34]	mode description
1	3720	3436	3500	3518	N3H stretch
2	3369	3123	3114	3160	C1H stretch, C2H stretch
3	3345	3073	3090	3135	C1H stretch, C2H stretch
4	3324	3073		3135	CH assym stretch
5	1552	1510	1524	1530	C1C2 stretch, N4C5 stretch
6	1525	1481	1483	1480	C5N3, C5H stretch
7	1490	1413	1415	1405	NC stretch, NH stretch
10	1196	1132	1132	1127	NC stretch

II. Im. An overall deviation of 0.53% from experiment was observed for neutral imidazole when compared to an FTIR experiment in an Ar matrix.[34] When compared to earlier experiments in the gas phase, the overall deviation from experiment was about 1.14%. We mention that these experiments include rotational effects which are not taken into account in our anharmonic calculations. Ab initio scaled VSCF showed exact agreement for the NC stretch modes when compared to matrix FTIR experiments. The majority of the calculated anharmonic frequencies had deviations below 0.3% (see Table 6). Overall, the agreement of scaled anharmonic VSCF frequencies to matrix experiment for neutral Im was better than the scaled VSCF frequencies for ImH^+. This could be due to the fact that the PM3 surface may not be as accurate for the charged species.

C. Nature of Anharmonic Effects. *1. Comparison of VSCF and Harmonic Frequency Deviations from Experiment.* Figure 3−d shows a comparison of percentage deviations from experiment for the calculated VSCF anharmonic frequencies and also percentage deviations of MP2 harmonic frequencies for the imidazole systems studied. We see the advantage of the anharmonic correction in reducing the error arising from the harmonic approximation consistently in all the species. As an example, in Figure 3a the advantage of applying the anharmonic correction is seen in $(ImH^+)(H_2O)N_2$ as the error due to using a harmonic approximation was reduced from 5% to 0.2% for the NH stretch modes. Similarly, the error due to the use of just a harmonic approximation for the CH stretch was reduced from 6% to an exact prediction with VSCF. We see that VSCF gives a consistent improvement over the harmonic prediction for vibrational modes with small and large anharmonicities.

The advantage of VSCF over the harmonic approximation is further highlighted in mode 2 of $(ImH^+)(H_2O)_2$ (Figure 3b). For this mode, harmonic frequencies exhibit a percentage deviation of 7% from experiment compared to 0.2% for VSCF anharmonic frequencies. For the hydrogen-bonded complexes, we see especially large corrections as we move from the harmonic to the anharmonic approximation particularly for the hydrogen-bonded stretch modes. This behavior can be attributed to the high anharmonicity inherent in hydrogen-bonded systems. We see an example in $(ImH^+)(H_2O)_2$, in which the water bound N4H stretch (mode 3) was corrected from an error of 11.7% in

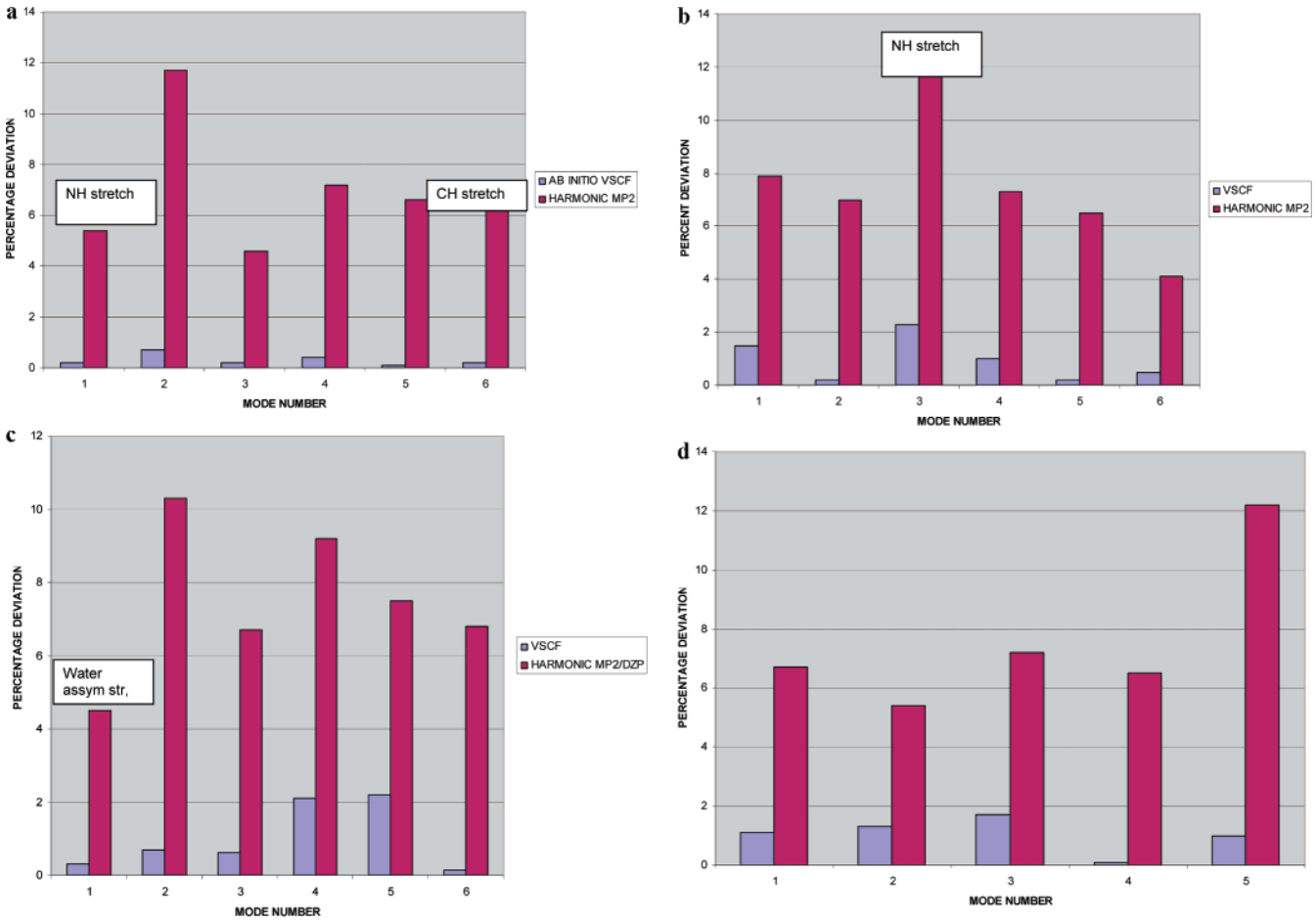

Figure 3. (a) Comparison of percentage deviations of ab initio frequencies of $(ImH^+)(H_2O)N_2$ and MP2 harmonic frequency calculations from experiment. (b) Comparison of percentage deviations of improved PM3 VSCF frequencies of $(ImH^+)(H_2O)_2$ and MP2 harmonic frequency calculations from experiment. (c) Comparison of percentage deviations of improved PM3 VSCF frequencies of $(ImH^+)H_2O$, and MP2 harmonic frequency calculations from experiment. (d) Comparison of percentage deviations of improved PM3 VSCF frequencies of ImH^+ and MP2 harmonic frequency calculations from experiment.

TABLE 7: $(ImH^+)(H_2O)N_2$ Comparison between ΔE_{diag} (in cm^{-1}) and ΔE_{coup} (in cm^{-1})

PM3 mode	MP2 (harm)	diag freq	VSCF (ab initio)	IRPD	$\lvert\Delta E\rvert_{diag}$	$\lvert\Delta E\rvert_{coup}$
1	3885	3799	3648	3639	86	151
2	4011	4104	3696	3723	93	408
3	3218	2964	2890	2897	253	74
4	3587	3422	3389	3404	115	33
5	3380	3290	3205	~3172	90	85
6	3372	3436	3165	~3172	64	331
7	3392	3344	3221	~3172	48	123

TABLE 8: $(ImH^+)(H_2O)_2$ Comparison between ΔE_{diag} cm^{-1} and ΔE_{coup} (in cm^{-1})

PM3 mode	MP2/DZP (harm)	diag freq	VSCF	IRPD	$\lvert\Delta E\rvert_{diag}$	$\lvert\Delta E\rvert_{coup}$
2	4012	3900	3776	3718	112	124
3	3890	3900	3642	3635	10	258
6	3240	3125	2967	2900	115	158
7	3402	3313	3202	~3170	89	111
8	3379	3378	3177	~3170	1	203

TABLE 9: ImH^+ Comparison between ΔE_{diag} cm^{-1} and ΔE_{coup} (in cm^{-1})

PM3 mode	MP2/DZP (harm)	diag freq	VSCF	IRPD[21]	$\lvert\Delta E\rvert_{diag}$	$\lvert\Delta E\rvert_{coup}$
1	3705	3488	3431	~3470	217	57
2	3660	3482	3424	~3470	178	58
3	3401	3330	3225	~3170	71	105
4	3379	3404	3174	~3170	25	230
5	3357	3206	3136	~3170	151	70

TABLE 10: Im Comparison between ΔE_{diag} cm^{-1} and ΔE_{coup} (in cm^{-1})

PM3 mode	MP2/DZP (harm)	diag freq	VSCF	FTIR expt[34]	$\lvert\Delta E\rvert_{diag}$	$\lvert\Delta E\rvert_{coup}$
1	3720	3436	3436	3500	284	0
2	3369	3197	3123	3114	171	74
3	3345	3091	3073	3090	254	18
5	1552	1530	1510	1524	22	20
6	1525	1491	1481	1483	34	10
7	1490	1445	1413	1415	45	32
10	1196	1187	1132	1132	9	55

the harmonic approximation to 2.3% in the anharmonic approximation. (Figure 3b).

The effect of anharmonic corrections to the water symmetric stretches proved to be very significant in the hydrogen-bonded complexes. This indicates the need for the inclusion of anharmonicity in the theoretical spectroscopy of biological molecules in a solvated environment approximation for biological processes which occur in solution. The importance of taking anharmonicity into account especially for solvated systems is seen in the water asymmetric stretch mode 1 of $ImH^+(H_2O)$, for which the introduction of anharmonicity reduces overall percentage error from 4.5% to 0.3%. (Figure 3c).

2. Comparison of Intrinsic and Coupling Anharmonicity. As mentioned previously, there are two different causes of anharmonic behavior, the intrinsic anharmonicity of the individual modes and the anharmonic coupling between different modes. The contribution of the intrinsic single mode anharmonicty (ΔE_{diag}) to the frequency is calculated as the difference between the frequency given by the diagonal potential $V_j^{diag}(Q_j)$ and the harmonic value of the frequency. On the other hand, the contribution of the anharmonic coupling element between modes (ΔE_{coup}) is computed as the difference between the VSCF value and the frequency value given by $V_j^{diag}(Q_j)$. Here we compare the values of ΔE_{diag} and ΔE_{coup}.

For $(ImH^+)(H_2O)N_2$ the absolute value of ΔE_{coup} is higher than that of ΔE_{diag} for most of the vibrational modes (Table 7). This indicates that for this system the contribution from anharmonic coupling between modes is greater than the contribution from single mode anharmonicities. The exception to this pattern in $(ImH^+)(H_2O)N_2$ are modes 3 and 4. When N_2 is replaced with water, the absolute value of ΔE_{coup} remains larger than that of ΔE_{diag} for all the modes examined (Table 8). For ImH^+ the contribution of single mode anharmonicity to the anharmonic character is greater for most modes. This is the case also with neutral imidazole (Tables 9 and 10). Thus, as hydrogen-bonding species are removed from the system the anharmonic character becomes more dependent on intrinsic single mode anharmonicities. We also observe that the anharmonic character for mode 1 (NH stretch) in ImH^+ changes from having a predominantly intrinsic character with some coupling character to a completely intrinsic character with no coupling characteristics whatsoever in neutral Im.

3. Magnitude of Anharmonic Coupling between Modes. From our analysis thus far, it is evident that spectroscopy is sensitive to anharmonic interactions in a given potential. Particularly, anharmonicity due to coupling between modes has an effect not only on frequencies but also on vibrational energy flow.[53] This effect happens to be paramount in hydrogen-bonded systems where anharmonicity due to coupling has a more significant effect than one-dimensional anharmonicities. An analysis of pairwise coupling effects in ImH^+ and its complexes with water may thus provide some insight into the nature of vibrational energy flow in nucleotides and nucleic acids. The average absolute value of the coupling potential was studied for ImH^+ and its complexes with water. Generally we observe coupling is non democratic.

In the case of the N_2 bound NH stretch (mode 4) in $ImH^+(H_2O)N_2$ intense coupling is observed between the NH stretch and the adjacent CH stretch (mode 5). This could be due to Fermi resonance between the modes that allows for energy transfer between modes. A very intense coupling of this mode is also observed however with mode 25 (NH in plane bending mode at 805 cm^{-1}). This coupling is due to the interaction of the NH stretch mode toward N_2 with the NH in plane bending mode. (See Figure 4a). Another interesting case is seen in the water bound NH stretch in $ImH^+(H_2O)_2$ where the most intense coupling is with modes 27 and 28, the lower frequency NH in plane bendings. This coupling character is similar to what is observed in $ImH^+(H_2O)N_2$ (see Figure 4b).

As an example of the nonbonded complexes, we consider coupling in ImH^+. For this isolated species, we see intense coupling between the NH stretch mode and also the NH in plane bending mode. We also see intense coupling between mode 3 (CH symmetric stretch) and mode 4 **(**CH asymmetric stretch**)**.

4. Im versus ImH$^+$. The main structural difference between neutral Im and ImH^+ lies in the presence of just one acidic NH group in neutral Im compared to two NH groups in ImH^+. We see that anharmoncity for the lone NH stretch group in neutral Im is completely due to intrinsic or diagonal anharmoncity with a $\lvert\Delta E\rvert_{diag}$ value of 284 cm^{-1} compared to 0 from $\lvert\Delta E\rvert_{coup.}$ This is not the case with the NH stretch modes of ImH^+ which have been noted by Andrei et. al to be weakly coupled with one another.[7] Although anharmonicity in the NH stretch modes of ImH^+ have a significant contribution from intrinsic anharmonicity there is also some contribution from mode−mode coupling. We see in the NH stretch modes of ImH^+ $\lvert\Delta E\rvert_{coup}$ values of 57 and 58 cm^{-1} compared to zero in neutral Im. Also, we noticed a slightly higher vibrational frequency in the NH

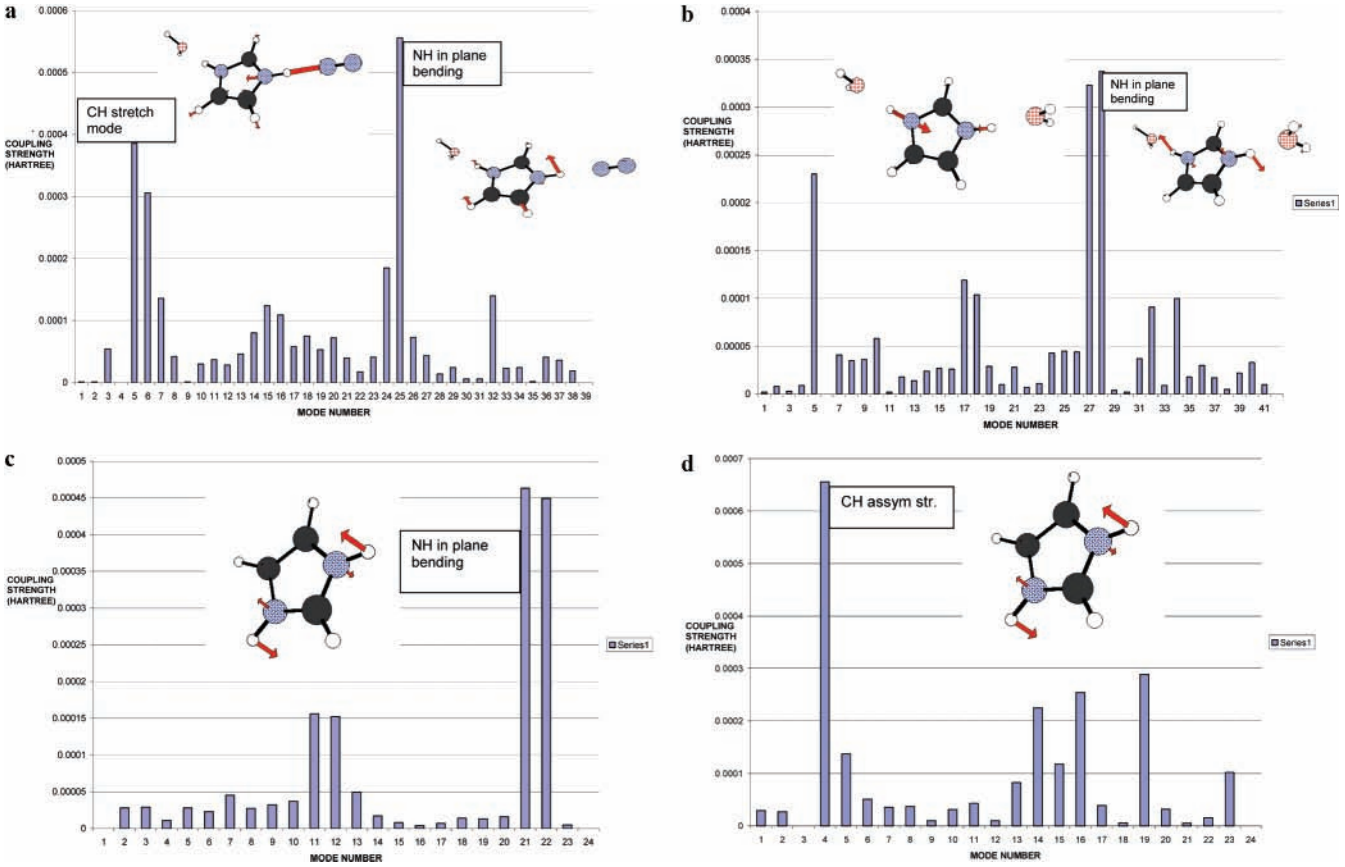

Figure 4. (a) Graph showing the integrated coupling potential between mode 4 of $(ImH^+)(H_2O)N_2$ (N_2 bound NH stretch) and other modes. (b) Graph showing the integrated coupling potential between mode 6 of $ImH^+(H_2O)_2$ (NH stretch) and other modes. (c) Graph showing the integrated coupling potential between mode 1 of ImH^+(NH stretch) and other modes. (d) Graph showing the integrated coupling potential between mode 3 of ImH^+(CH stretch) and other modes.

stretch mode of 3436 cm^{-1} in neutral Im compared to 3431 cm^{-1} in ImH^+. This can be attributed to the reduced effect of mode−mode coupling on the NH stretch mode in neutral Im. As we move from ImH^+ to neutral Im, we see an increase in percentage anharmonicity especially for the NH stretch and CH stretch modes in neutral Im. Percentage anharmonicity for the NH stretch mode is observed to increase from about 7.9% in ImH^+ to about 8.2% in neutral Im. Similarly, the percentage anharmonicity is observed to increase in the CH stretch modes as we move from ImH^+ (5.4% and 6.4%) to neutral Im (7.8% and 8.8%). This analysis provides some insight into the variation in anharmonic character of the PES of ImH^+ and neutral Im.

Conclusion

We have calculated the anharmonic vibrational spectra of neutral imidazole, protonated imidazole and its complexes with water. The results from the VSCF calculations carried out on an ab initio improved PM3 surface provide a detailed view into anharmonicity and its accompanying effects in this essential biomolecular building block. The theoretical-experimental analysis shows that the explicit inclusion of anharmonic effects is very important for achieving agreement between theory and experiment as anharmonic frequencies obtained from VSCF calculations are of remarkable similarity to experiment. This agreement between theory and experiments validates the PES and encourages the use of high level ab initio methods not only in the theoretical spectroscopy of biological systems but also in applications such as molecular dynamics simulations. We also observe that with adequate scaling PM3 is indeed able to describe hydrogen-bonded complexes to a high degree of accuracy. This is important as PM3 is much faster than pure ab initio methods and its efficient use will make the anharmonic treatment of large biological molecules possible.

In addition, we have found that both intrinsic anharmonicities of single modes as well as coupled anharmonicities play an important role in ImH^+ and its complexes. In particular, we have noticed that anharmoncity in hydrogen-bonded species such as $(ImH^+)(H_2O)N_2$ and $(ImH^+)(H_2O)_2$ is mainly due to coupling between modes. This coupled anharmonicity changes to a more intrinsic character as hydration is reduced. Similarly, we see that the NH stretch mode of neutral Im has no coupling character while that of ImH^+ has some coupled characteristics. We also observe that the percentage anharmonicity in the NH stretch and CH stretch modes differ greatly in neutral Im and ImH^+. In this study we also characterized the coupling between different normal modes. The results show that the magnitude of anharmonic couplings between different pairs of normal modes depends very selectively on the modes involved. Vibrational energy transfer and redistribution in polyatomic molecules is due to anharmonic couplings between different modes. The findings on these couplings may hopefully motivate future experimental and theoretical studies on energy flow in these systems.

Acknowledgment. We are grateful to Dr. Erick Fredj and Dr. Brina Brauer for their assistance and for kindly providing the ab initio scaling code. The research at the Hebrew University of Jerusalem was supported by a grant from the US-Israel Binational Science Foundation (BSF 2004009). The experi-

mental research was supported by the *Deutsche Forschungsgemeinschaft* (DO 729/2) and the *Fonds der Chemischen Industrie*.

Supporting Information Available: List of bond lengths. This material is available free of charge via the Internet at http://pubs.acs.org.

References and Notes

(1) Stryer, L. *Biochemistry*; Freeman: New York, 1996.
(2) Noguchi, T.; Inoue, Y.; Tang, X. *Biochemistry* **1999**, *38*, 399.
(3) Garczarek, F.; Brown, L. S; Lanyi, J. K; Gerwerk, K. *Proc. Natl. Acad. Sci.* **2005**, *102*, 3633.
(4) Meyer, E. A.; Castellano, R. K.; Diedrich, F. *Angew. Chem.* **2003**, *115*, 1244.
(5) Choi, M. Y.; Miller, R. E. *J. Phys. Chem. A* **2006**, *110*, 9344−9351.
(6) Andrei, H-S.; Solca, N.; Dopfer, O. *J. Phys. Chem. A* **2005**, *109*, 3598.
(7) Andrei, H-S.; Solca, N.; Dopfer, O. *Chem. Phys. Chem.* **2006**, *7*, 107−110.
(8) Scheiner, S.; Kar, T.; Pattanayak, J. *J. Am. Chem. Soc.* **2002**, *124*, 13257−13264.
(9) Bu, Y. X.; Cukier, R. I. *J. Phys. Chem. B* **2004**, *108*, 1008.
(10) Choi, M. Y.; Miller, R. E. *J. Am. Chem. Soc.* **2006**, *128*, 7320.
(11) Choi, M. Y.; Douberly, G. E.; Falconer, T. M.; Lewis, W. K.; Lindsay, C. M.; Merritt, J. M.; Stiles, P. L.; Miller, R. E. *Int. Rev. Phys. Chem.* **2006**, *25*, 15.
(12) Choi, M. Y.; Miller, R. E. *Phys. Chem. Chem. Phys.* **2005**, *7*, 3565.
(13) Choi, M. Y.; Dong, F.; Miller, R. E. *Phil. Trans. R. Soc. London, Ser. A* **2005**, *363*, 393.
(14) Oomens, J.; Von Helden, G.; Meijer, G. *J. Phys. Chem. A* **2004**, *108*, 8273.
(15) Oh, H.-B.; Lin, C.; Hwang, H. Y.; Carpenter, B. K.; Mclafferty, F. W. *J. Am. Chem. Soc.* **2005**, *127*, 4076.
(16) Lucas, B.; Gregoire, G.; Lemaire, J.; Maitre, P.; Glotin, F., Scherman, J. P.; Desfrancois, C. *Int. J. Mass Spectrom.* **2005**, *243*, 105.
(17) Macleod, N. A.; Simons, J. P. *Phys. Chem. Chem. Phys.* **2004**, *6*, 2821−2826.
(18) Solca, N.; Dopfer O. *Angew. Chem.* **2003**, *115*, 1575.
(19) Snoek, L. C.; Robertson, E. G.; Kroemer, R. T. Simons, J. P. *Chem. Phys. Lett*. **2000**, *321*, 49.
(20) Carcabal, P.; Kroemer, R. T.; Snoek, L. C.; Simons, J. P.; Bakker, J. M.; Compagnon, I.; Meijer, G.; von Helden, G. *Phys. Chem. Chem. Phys.* **2004**, *6*, 4546.
(21) Cohen, R.; Brauer, B.; Nir, E.; Grace, L.; de Vries, M. S. *J. Phys. Chem. A* **2000**, *104*, 6351.
(22) Nir, E.; Kleinermanns, K.; de Vries, M. S. *Nature* **2000**, *408*, 949.
(23) Plutzer, C.; Meijer, G.; von Helden, G.; Kabelac, M.; Hobza, P.; de Vries, M. S. *Chem. Phys. Chem.* **2003**, *4*, 838.
(24) Bakker, J. M.; Compagnon, I.; Meijer, G, von Helden, G.; Kabelac, M.; Hobza, P.; de Vries, M. S. *Phys. Chem. Chem. Phys.* **2004**, *6*, 2810.
(25) Abo-riziq, A.; Crews, B. O.; Callahan, M. P.; Grace, L.; de Vries, M. S. *Angew. Chem., Int Ed.* **2006**, *45*, 5166.
(26) Linder, R.; Nispel, M.; Haber, T.; Kleinermanns, K *Chem. Phys. Lett.* **2005**, *409*, 260.
(27) Abo-riziq, A.; Bushnell, J. E.; Crews, B.; Callahan, M.; Grace, L.; de Vries, M. S. *Chem. Phys. Lett*. **2006**, *431*, 227.
(28) Toroz, D.; van Mourik, T. *Mol. Phys.* **2006**, *104*, 559.
(29) Gerlach, A.; Unterberg, C.; Fricke, H.; Gerhards, M. *Mol. Phys.* **2005**, *103*, 1521.
(30) Compagnon, I.; Oomens, J.; Meijer, G.; von Helden, G. *J. Am. Chem. Soc*. **2006**, *128*, 3592.
(31) Chin, W.; Piuzzi, I. F.; Dimicolli, I.; Mons, M. *Phys. Chem. Chem. Phys.* **2006**, *8*, 1033.
(32) Solca, N.; Dopfer O. *Chem. Phys. Chem.* **2005**, *6*, 434.
(33) Simons, J. P. *Phys. Chem. Chem. Phys.* **2004**, *6*, E7.
(34) Van Bael, M. K.; Smets, J.; Schoone, K.; Houben, L.; Mccarthy, W.; Adamowicz, L.; Novak, M. J.; Maes, G. *J. Phys. Chem. A* **1997**, *101*, 2397−2413., King, S. T. *J. Phys. Chem.* **1970**, *74*, 2133.
(35) Jung, J. O.; Gerber, R. B. *J. Chem. Phys.* **1996**, *105*, 10332−10348.
(36) Gregurick, S. K.; Chaban, G. M.; Gerber, R. B. *J. Phys. Chem. A* **2002**, *106*, 8696−8707.
(37) Brauer, B.; Chaban, G. M.; Gerber, R. B. *Phys. Chem. Chem. Phys.* **2004** *6*, 2543−2556.
(38) Chaban, G. M.; Jung, J. O.; Gerber, R. B. *J. Chem. Phys.* **1999**, *111*, 1623−1629.
(39) Matsunaga, N.; Chaban, G. M.; Gerber, R. B. *J. Chem. Phys*. **2002**, *117*, 3541−3547.
(40) Adesokan, A. A.; Fredj, E.; Brown, E. C.; Gerber, R. B. *Mol. Phys.* **2005**, *103*, 1505−1520.
(41) Miller, Y.; Chaban, G. M.; Gerber, R. B. *J. Phys. Chem. A* **2005**, *109*, 6565−6574.
(42) Benoit, D. M. *J. Chem. Phys.* **2004**, *120*, 562−573.
(43) Schmidt, M. W.; Baldridge, K. K.; Boatz, J. J.; Elbert, S. T.; Gordon, M. S.; Jensen, J. J.; Koseki, S.; Matsunaga, N.; Nguyen, K. A.; Su, S.; Windus, T. L.; Dupuis, M.; Montgomery, J. A. *J. Comput. Chem.* **1993**, *19*, 1347−1363.
(44) Brauer, B.; Gerber, R. B.; Kabelac, M.; Hobza, P.; Bakker, J. M.; Abo Riziq, A. G.; deVries, M. S. *J. Phys. Chem. A* **2005**, *109*, 6974−6984.
(45) Stewart, J. J. P. *J. Comput. Chem*. **1989**, *10*, 209−220.
(46) Pople, J. A.; Binkley, J. S.; Seeger, R. *Int. J. Quantum Chem*. **1976**, *10*, 1.
(47) Dunning, T. H. *J. Chem. Phys.* **1971**, *55*, 716.
(48) Dunning, T. H.; Hay, P. J. In *Methods of Electronic Structure Theory* ; Schaefer, H. F., Ed. ; Plenum: New York, 1977; Chapter 1, pp 1−27.
(49) Bode, B. M.; Gordon, M. S. *J. Mol. Graph. Modeling* **1998**, *16*, 133−138.
(50) Dopfer, O. *Int. Rev. Phys. Chem*. **2003**, *22*, 437.
(51) Harb, W.; Bernal-Uruchurtu, M. I.; Ruiz-Lopez, M. F. *Theor. Chem. Acc.* **2004**, *112*, 204−216.
(52) Dannenberg, J. J. *THEOCHEM* **1997**, *401*, 279−286.
(53) Leitner, D. *J. Phys. Chem. A* **1997**, *101*, 547−548.